S7-2   Frequency Agile Bandpass Filter for Direct Detection Lidar Receivers

William J. Marinelli, Christopher M. Gittins, and William G. Lawrence

Physical Sciences Inc.
20 New England Business Center, Andover, MA 01810
marinelli@psicorp.com; Voice: 978.689.0003; FAX: 978.689.3232

In this paper we discuss the use of a tunable IR filter based on a low-order Fabry-Perot etalon to sharply reduce the instantaneous spectral response width of a DIAL detection system. This approach reduces the background-limited radiative flux reaching the detector, thus providing an increased value of the specific detectivity, D^*. When other sources of detector system noise are considered, the overall improvement in noise equivalent power ranges from 2 to almost 7, depending on the characteristics of the environment being probed. The improvement in D^* was accomplished while maintaining the capability of a CO_2 laser based DIAL system to access the full range of lines available from a tunable laser transmitter. (The spectral tuning rate of the prototype filter described here approaches 2000 cm^{-1} per second.)

The signal-to-noise ratio (SNR) of a lidar measurement is limited by laser speckle noise as well as the intrinsic noise characteristics of the detector and amplifier. For a two-wavelength dial-based species column density measurement conducted at long ranges or for weak laser sources, where $SNR_{det} \ll SNR_{speckle}$, and where the plume is larger than the laser spot size, the standard deviation of the column density is given by [1]:

$$\sigma_{<CL_{plume}>} = \frac{1}{2\rho \left(\sqrt{N} \times SNR_{det} \right)}$$ (1)

where ρ is the differential absorption coefficient of the species under investigation at the two wavelengths and N is the number of laser shots averaged. The detector SNR is defined as the ratio of the return signal power to the detector noise equivalent power. In the absence of atmospheric sources of noise, SNR_{det} for a direct detection DIAL system with a topographic target is given by:

$$SNR_{det} = \left(\frac{\epsilon P_{AV}}{N_D \gamma \, prf} \right) \times \frac{D^*}{\sqrt{A_D \gamma^{-1}}} \times \left(\frac{d_{rec}^2}{4L^2} \right) r \, \exp[-2KL]$$ (2)

where ϵ is the optical efficiency, P_{AV} is the average transmitted laser power, N_D is the number of detectors (if an array is used), prf is the laser pulse repetition frequency, D^* is the detectivity, A_D is the detector area, γ is the laser pulse width, d_{rec} is the receiver diameter, L is the target range, r is the target albedo, and K is the atmospheric attenuation coefficient. Combining Eqs. (1) and (2) we find that $\sigma_{<CL>}$ is inversely proportional to D^*, i.e. larger values of D^* reduce linearly the uncertainty in the concentration measurement.

The baseline performance of an IR detector is described by its specific detectivity, D^* (Reference 2). The value of D^* for background limited detection is given by the expression:

$$D_{BLIP}^*(\lambda, \theta_{1/2}) = \frac{\lambda}{hc} \eta(\lambda) \left[2 \sin^2\theta_{1/2} \int_0^{\lambda_{max}} \eta(\lambda) M_p(\lambda, T_B) \, d\lambda \right]^{-1/2} ,$$ (3)

where $\eta(\lambda)$ is the detector quantum efficiency, $\theta_{1/2}$ is the half-angle field of view, and M_p is the blackbody spectral radiant flux exitance given by the expression:

$$M_{P,\lambda}(\lambda,T) = \frac{2\pi \ c \ \epsilon(\lambda)}{\lambda^4[\exp(hc/\lambda kT) - 1]} \tag{4}$$

where T is the blackbody temperature of the field-of-view and $\epsilon(\lambda)$ is the wavelength dependent emissivity, which is nearly constant and close to unity in the LWIR spectral region. In practice, we modify the integrand in Eq.(4) to include the transmission of the coupling optics and their self-radiance.

In this investigation we explored the use of a low-order Fabry-Perot etalon to reduce the instantaneous spectral response bandwidth of a prototype lidar receiver. For coverage of the long wavelength infrared (LWIR) spectral region, we operate the interferometer in third order $m_{max} = 3$ such that the mirror spacing is approximately 1.5 times the desired transmission wavelength. In the absence of significant reflected phase dispersion, the free spectral range (FSR), corresponding to the range of mirror motion (wavelength tuning) possible before orders recur, is given by the expression:

$$\Delta\lambda_{FSR} = \frac{\lambda_{max}}{m_{max} + 1} \tag{5}$$

where λ_{max} is the highest transmitted wavelength desired. The theoretical FSR for a system operating in m = 3 with a maximum wavelength of 11.1 μm (DIAL system maximum) is 2.78 μm. However, for the mirror set used in the interferometer available for these measurements, reflected phase effects in the coating reduce the effective FSR to approximately 1.9 μm. At an achievable finesse level of approximately 25, the system is capable of a spectral resolution of approximately 7 to 9 cm^{-1}.

Common experience holds that, to improve detector D^*, a filter must be cooled to reduce thermal radiance. However, Fabry-Perot interferometers are reflective optics and cryogenic operation of the filter module is not required to obtain much of the SNR improvement anticipated as a result of this approach. The etalon itself has an emissivity of ~0.01 averaged over the passband of the cold filter. This emissivity corresponds to an apparent field temperature of ~ 150 K. In contrast, an absorbing or scattering filter has near unit emissivity outside of its passband and its field temperature is equal to its thermodynamic temperature. When placed in an afocal region of the optical train, the interferometer re-images the 77 K detector on to itself and detector self-radiance provides a minimal contribution to the baseline flux level.

The optical layout of the system used to evaluate this concept comprises a 19 mm f/1.45 lens system coupled to a (0.5 mm)^2 mercury cadmium telluride (MCT) photoconductive detector. The FOV of the detector is determined by a specially fabricated cold shield, designed to match the f-number of the collection optics. A 10.0 to 11.0 μm bandpass filter (58% peak transmission) is mounted on the cold shield to define the primary detection bandpass of the system. The detector was manufactured by Kolmar Inc., with a nominal D^* of 5×10^{10} cm Hz$^{1/2}$ W^{-1} (Jones) at 300 K (60° cold shield) and a nominal responsivity of 1.37×10^4 V/W. The interferometer is close coupled to the cooled lens assembly input window on a common optical axis. The entire assembly is coupled to the large aperture chopper, which passed the entire FOV of the optical system. The chopper is used in conjunction with a lock-in amplifier to measure the absolute responsivity of the detection system. Noise measurements are performed by staring at a high temperature extended source blackbody, which filled the field-of-view of the tunable filter/cooled lens/detector assembly.

The response of the system is determined by recording the detector signal as a function of blackbody temperature, both with and without the interferometer inserted into the optical train. The detector noise equivalent power (NEP) is calculated from the voltage fluctuations measured over the frequency range from 10 to 30 kHz and related to the system D^* using the expressions:

$$NEP = \frac{N_v}{R} \qquad D^* = \frac{\sqrt{A \times \Delta f}}{NEP} \tag{6}$$

where N_v is the RMS voltage noise and R is the measured detector responsivity (V/W). Figure 1 shows how the NEP of the system varies as a function of field temperature from approximately 400 to 900 K, with and without the interferometer present. The data clearly shows a decrease in the NEP with the insertion of the interferometer as well as the slow increase in NEP as a function of temperature, consistent with a system operating near the background limit. The ratio of the NEP values gives the D^* improvement afforded by the insertion of the tunable filter into the optical train. This ratio, shown on the right axis of Figure 1, is 4.18 ± 0.62 (2σ) and is independent of temperature, within the error limits of the data. The uncertainty in the ratio increases as the temperature decreases because the uncertainty associated with measuring the NEP with the etalon inserted into the optical train. At ambient temperature the amplifier noise in this system is significantly greater than the detector noise. Accordingly, we report the D^* improvement at 500 K (20 kHz center frequency) in accordance with the convention of reporting D^* at that same temperature.

The measured improvement in D^* can be compared with the expected improvement based on a background limited detector. A model was exercised for the conditions of the experimental measurement and validated by comparison with the data reported for the detector by the manufacturer. Our system model, which uses ideal theory and assumes BLIP limited noise, overpredicts the measured D^* by approximately 50%. Such a disagreement is not unusual and simply indicates that the detector was not operating at the theoretical limit of performance. The difference is well within the range of expected performance. Figure 2 shows the measured D^* values obtained in these measurements as well as the variation in D^* predicted from the model and multiplied by a single scale factor for comparison. The model D^* calculations accurately predict the trend in D^* with temperature and the single scale factor accurately adjusts the calculation to agree very well with the data under all conditions. The D^* improvement ratio obtained from the model is also independent of temperature and has a value of 3.98. Thus, the measured D^* improvement agrees very well with the model predictions and shows that this approach is capable of achieving the theoretical D^* improvement ratio. Note that the improvement ratio calculated from the model is independent of the absolute magnitude of the system D^* and only dependent on the ratio of system spectral bandwidths. The good agreement between the model and the experimental data validates the model and allows us to use it to predict system performance for a candidate DIAL system.

The system model was exercised to simulate and predict the performance of a lidar receiver incorporating this technology. The model predicts the overall improvement in system D^* as a function of adding the tunable filter, other detector system noise constraints do not allow the full realization of the improvement. We can capture the nature of this effect by considering the improvement in total system noise equivalent power (NEP) as a function of both detector type and size as well as and preamplifier noise. The effect is illustrated in Figure 9 where we have included detector bias current and Johnson noise and assumed a preamplifier with a gain of 10 and an input noise voltage of 0.5 nV Hz$^{-1/2}$. The effective amplifier NEP is calculated using a responsivity of 1.4×10^4 V/W and summed, assuming Gaussian additive noise sources, with the detector NEP calculated using the standard expressions. The curve shows an asymptotic approach to the effective amplifier NEP as the detector D^* improves. We can place expected system performance improvement on this curve considering two scenarios, one in which the target field is at a temperature of 300 K (ambient) and one in which the target field is at 500 K. The symbols on the curve show the system NEP for four cases. The solid square symbol shows the system NEP calculated for the basic receiver at its nominal D^* for a field at 300 K. The solid circle shows the NEP for the addition of the tunable filter to the receiver viewing the 300 K field. The resulting improvement in NEP is 2.0. Thus, the anticipated improvement in receiver D^* calculated based on the detector alone must be derated to this factor of roughly 2. If the field temperature is increased to 500 K the existing receiver system is calculated to have an NEP given by the open square symbol. Adding the tunable filter under those conditions gives an NEP depicted by the open circle. This situation gives a practical improvement in NEP (and hence effective D^*) of 6.9. Thus, the total system improvement depends not only on the optical system but also on the method of deployment.

The measurements reported in this paper demonstrate that the insertion of a low-order tunable etalon into the optical train of a CO_2 laser lidar receiver can provide significant detector performance enhancements. The incorporation of the etalon into the receiver reduces system noise by reducing the instantaneous spectral bandwidth of the IR detector to a small wavelength range centered on the transmitted CO_2 laser line, thereby improving the overall D^* of the detection system. This improvement in D^* is accomplished using a tunable filter which enables the system to switch wavelengths up to 300 times per second with less than 2% variation in receiver transmission from pulse to

pulse. The concept was demonstrated experimentally, achieving the full theoretically possible increase in D^*. A consideration of overall detector system performance results in a projected factor of 2 to 7 in noise reduction. Lidar theory indicates that, for a fixed return power and a system limited by detector noise, system range increases as the square root of the signal-to-noise ratio improvement while the signal-to-noise ratio improves linearly with improvement in D^*. These improvements can play a key role in the ability of DIAL to monitor airborne chemicals from long standoff distances.

REFERENCES

1. Harney, R.C., "Laser prf considerations in differential absorption lidar applications," Appl. Opt. 22, 3747-3750 (1983).
2. Rogatto, W.D. Ed., The Infrared and Electro-Optical Systems Handbook: Vol. 3, Electro-Optical Components, SPIE Optical Engineering Press, Bellingham, WA, 1993, pp. 220-227.
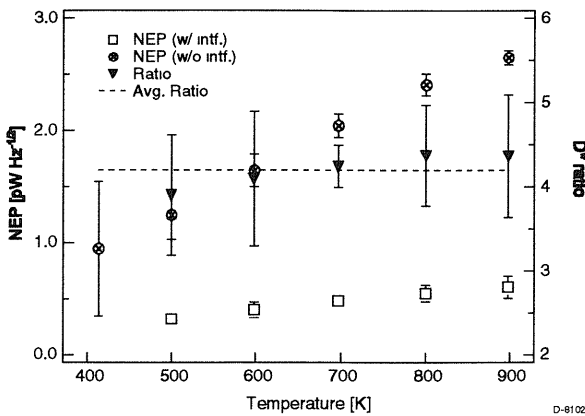
Figure 1. Measured NEP with and without the interferometer present and D^* improvement ratio calculated from the data. The average D^* improvement is given by the horizontal dotted line. Error bars are 2σ.
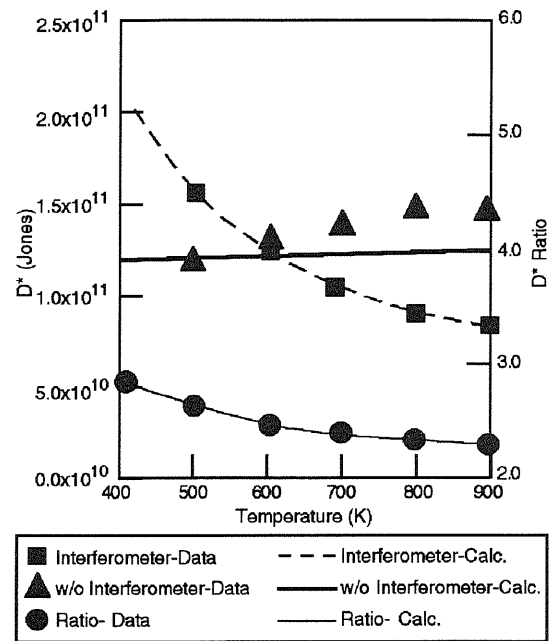

Figure 2. Measured and calculated(scaled) D^* as a function of temperature with and without the interferometer present in the optical train.
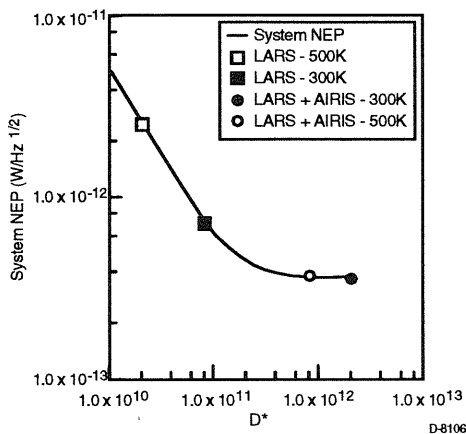

Figure 3. Variation in amplifier/detector noise equivalent power as a function of detector D^* for the basic receiver and the receiver with the tunable filter.